Molecular Biology of the Cell
Vol. 17, 1410–1420, March 2006

PGAP2 Is Essential for Correct Processing and Stable Expression of GPI-anchored Proteins[D]

Yuko Tashima,* Ryo Taguchi,† Chie Murata,† Hisashi Ashida,* Taroh Kinoshita,* and Yusuke Maeda*

*Department of Immunoregulation, Research Institute for Microbial Diseases, Osaka University, Suita, Osaka 565-0871, Japan; and †Department of Metabolome, Graduate School of Medicine, The University of Tokyo, Tokyo 113-0033, Japan

Submitted November 2, 2005; Revised December 27, 2005; Accepted January 4, 2006
Monitoring Editor: Howard Riezman

Biosynthesis of glycosylphosphatidylinositol-anchored proteins (GPI-APs) in the ER has been extensively studied, whereas the molecular events during the transport of GPI-APs from the ER to the cell surface are poorly understood. Here, we established new mutant cell lines whose surface expressions of GPI-APs were greatly decreased despite normal biosynthesis of GPI-APs in the ER. We identified a gene responsible for this defect, designated PGAP2 (for Post-GPI-Attachment to Proteins 2), which encoded a Golgi/ER-resident membrane protein. The low surface expression of GPI-APs was due to their secretion into the culture medium. GPI-APs were modified/cleaved by two reaction steps in the mutant cells. First, the GPI anchor was converted to lyso-GPI before exiting the *trans*-Golgi network. Second, lyso-GPI-APs were cleaved by a phospholipase D after transport to the plasma membrane. Therefore, PGAP2 deficiency caused transport to the cell surface of lyso-GPI-APs that were sensitive to a phospholipase D. These results demonstrate that PGAP2 is involved in the processing of GPI-APs required for their stable expression at the cell surface.

INTRODUCTION

The glycosylphosphatidylinositol (GPI)-anchor is conserved among eukaryotes. To date, more than 150 different proteins in mammalian cells have been identified as GPI-anchored proteins (GPI-APs). The backbone of the GPI anchor consists of ethanolamine phosphate, three mannoses, glucosamine and phosphatidylinositol (PI) (Ferguson, 1999; Kinoshita and Inoue, 2000; Ikezawa, 2002). The GPI anchor is assembled on PI and transferred to proteins in the ER. Newly synthesized GPI-APs are transported to the plasma membrane by vesicular trafficking. GPI-APs are concentrated in microdomains in the plasma membrane, so-called rafts, which are enriched with cholesterol and sphingolipids (Brown and Rose, 1992; Simons and Ikonen, 1997; Simons and Toomre, 2000). GPI-APs are incorporated into rafts in the Golgi during their transport to the cell surface (Brown and Rose, 1992). The rafts are thought to act as signaling platforms in which molecules are assembled according to extracellular stimuli and transduce raft-dependent intracellular signals (Brown and Rose, 1992; Simons and Ikonen, 1997; Simons and Toomre, 2000), to mediate apical sorting of GPI-APs in epithelial cells (Brown and Rose, 1992; Mayor and Riezman, 2004; Paladino *et al.*, 2004), and to regulate the endocytic trafficking (Chatterjee *et al.*, 2001; Mayor and Riezman, 2004). Therefore, it is important to clarify the mechanisms by which GPI-APs are transported to the cell surface and integrated into rafts.

The GPI biosynthetic pathway has been extensively studied and many of the genes involved have been identified in mammalian, yeast, and other systems (Kinoshita and Inoue, 2000). On the other hand, little is known, especially in mammalian cells, about which molecules and transport vesicles mediate the transport of GPI-APs and their integration into rafts. In yeast, GPI-APs are transported in ER-derived vesicles that differ from those for other secretory proteins, and the Rab GTPase Ypt1p and tethering factors Uso1p, Sec34p, and Sec35p are required for sorting of GPI-APs upon their exit from the ER (Morsomme and Riezman, 2002; Morsomme *et al.*, 2003). The cargo receptor molecules Emp24p, Erv25p, and their family members are also required for efficient sorting and transport of GPI-APs (Schimmoller *et al.*, 1995; Muniz *et al.*, 2000). Moreover, trafficking of GPI-APs from the ER to the Golgi requires ongoing ceramide synthesis (Skrzypek *et al.*, 1997; Sutterlin *et al.*, 1997). In mammalian cells, several cholesterol and sphingolipid depletion experiments have indicated the importance of their association with rafts for the endocytic pathway of GPI-APs (Mayor *et al.*, 1998; Chatterjee *et al.*, 2001; Mayor and Riezman, 2004). VIP17/MAL is the only molecule known to interact biochemically with GPI-APs and is required for apical sorting of GPI-APs in polarized cells (Cheong *et al.*, 1999; Martin-Belmonte *et al.*, 2000). Studies of cells from caveolin-1 knockout mice have revealed that caveolin-1 affects the distribution of GPI-APs (Sotgia *et al.*, 2002). Thus, the sorting mechanism for GPI-APs is unique and specific, presumably due to the characteristics of GPI.

This article was published online ahead of print in *MBC in Press* (http://www.molbiolcell.org/cgi/doi/10.1091/mbc.E05–11–1005) on January 11, 2006.

[D] The online version of this article contains supplemental material at *MBC Online* (http://www.molbiolcell.org).

Address correspondence to: Yusuke Maeda (ymaeda@biken.osaka-u.ac.jp) or Taroh Kinoshita (tkinoshi@biken.osaka-u.ac.jp).

Abbreviations used: BFA, brefeldin A; CHO, Chinese hamster ovary; GPI-AP, glycosylphosphatidylinositol-anchored protein; PGAP, post-GPI-attachment to proteins; PLA, phospholipase A; PLD, phospholipase D; TGN, *trans*-Golgi network.

We have been studying genes that play roles in GPI-AP transport and behavior on the cell surface. Previously, we reported one such gene, designated PGAP1 (Post-GPI-Attachment to Proteins 1; Tanaka *et al.*, 2004). PGAP1 is a deacylase that removes a palmitate from the inositol of GPI-APs in the ER immediately after attachment of GPI to proteins. In PGAP1-deficient cells, transport of GPI-APs from the ER to the Golgi was delayed (Tanaka *et al.*, 2004). Here, we report the establishment of new mutant cell lines whose surface expressions of GPI-APs were greatly decreased despite normal biosynthesis of GPI-APs in the ER, and the identification of the PGAP2 gene responsible for this defect. Analyses of the mutant phenotype provide further insights into the mechanisms by which GPI-APs are correctly processed during transport and expressed on the cell surface.

MATERIALS AND METHODS

Cells and Culture

3B2A, 3B2A-GD3S C37, C84*, C84, AM-B, and BTP2 cells were cultured in Ham's F12 medium (Sigma, St. Louis, MO) supplemented with 10% fetal calf serum (FCS), 0.4 mg/ml G418 and appropriate antibiotics as described below. NRK cells were cultured in DMEM (Sigma) supplemented with 10% FCS. Serum-free medium-adapted cells were cultured in CHO-S-SFM II (Invitrogen, Carlsbad, CA) on dishes coated with collagen (Iwaki, Tokyo, Japan). C84* cells were derived from the Chinese hamster ovary (CHO) cell line 3B2A-GD3S and defective in PGAP2 and UDP-galactose transporter (UGT; see Supplementary Information for the generation and characterization of C84* cells).

Cloning of PGAP2 cDNA

C84* cells (3×10^8) were suspended in 4 ml of Opti-MEM I (Invitrogen) containing 300 μg each of a rat C6 glioma cDNA library and pcDNA-PyT (ori-) plasmids (Nakamura *et al.*, 1997), divided into 10 cuvettes and electroporated at 280 V and 960 μF using a Gene Pulser (Bio-Rad, Richmond, CA). At 2 d after the transfection, the cells were stained with a biotinylated anti-CD59 antibody and phycoerythrin-conjugated streptavidin. Cells with restored surface expression of CD59 were collected by a cell sorter. Plasmids were recovered from these cells by Hirt's method (Hirt, 1967). After another cycle of cell sorting and plasmid recovery, we analyzed 960 clones and obtained 1 positive clone. The rat UGT gene was also identified by a similar expression cloning experiment based on the restoration of GD3 expression on C84* cells.

To clone hamster PGAP2, a partial cDNA fragment was amplified by PCR from a CHO cDNA library (a gift from Dr. O. Kuge, Kyushu University) using the degenerate primers deF1 (5′-GCCTTCGCCTAYTGGAAYCAYTA) and deR1 (5′-TCCCACCAGGCYGTCATRTGRAA). Based on this amplified sequence, hamster PGAP2-specific primers were designed. The remaining 5′ and 3′ regions of the cDNA were amplified by nested-PCR using vector- and PGAP2-specific primers.

FACS Analyses for GPI-APs and Transmembrane Proteins

AM-B cells were cotransfected with either a mock or PGAP2 expression vector and the indicated plasmids. Cells (5×10^6) were suspended in 0.4 ml of Opti-MEM I and electroporated with 10 μg of each of the plasmids at 260 V and 960 μF using a Gene Pulser. FLAG-tagged-CD59-TM was produced by replacing the GPI attachment signal with the transmembrane (TM) domain of CD46 (Hong *et al.*, 2002). At 2 d after the transfection, the cells were stained with mouse anti-FLAG M2 (Sigma), mouse anti-placental alkaline phosphatase (PLAP; Sigma), mouse anti-CD25 (BD Biosciences, San Jose, CA) or mouse anti-P75 antibodies (Cell Resource Center for Biomedical Research, Institute of Development, Aging and Cancer, Tohoku University) followed by an FITC-conjugated anti-mouse IgG antibody, and analyzed by FACS.

Immunofluorescence Microscopy

NRK cells in 0.4 ml of Opti-MEM I were electroporated with 10 μg each of plasmids containing rat PGAP2 cDNA and myc-tagged DPM2 at 250 V and 960 μF using a Gene Pulser. Cells were incubated with or without 5 μg/ml BFA (MP Biomedicals, Irvine, CA) for 10 min, and then fixed with 4% paraformaldehyde in phosphate-buffered saline (PBS) for 15 min. After quenching with 40 mM ammonium chloride in PBS, the cells were permeabilized with PBS containing 0.1% Triton-X (TX)-100 and 2.5% goat serum for 1 h at room temperature and stained with rabbit anti-PGAP2, mouse anti-GM130 (BD Biosciences) or mouse anti-myc (9E10) antibodies followed by an Alexa 488-conjugated donkey anti-mouse IgG antibody (Molecular Probes, Eugene, OR) or Alexa 594-conjugated goat anti-rabbit IgG antibody (Molecular Probes). The hybridoma producing the 9E10 antibody was obtained from the Developmental Studies Hybridoma Bank developed under the auspices of the National Institute of Child Health and Human Development and maintained by the Department of Biological Sciences, University of Iowa. The rabbit anti-PGAP2 serum was raised against the C-terminal peptide (DFGNKELLITSQPEEKRF) that is conserved among hamsters, rats, mice, and humans. The pictures were taken by BX50 microscope (Olympus, Tokyo, Japan) and VB-6010 CCD camera (Keyence, Osaka, Japan).

Subcellular Fractionation

We established AM-B cells that were responsive to doxycycline by stable cotransfection with pTRE2-puro-rat PGAP2, constructed by subcloning rat PGAP2 into the pTRE2pur vector (BD Biosciences), and pUHrT 62–1 (a gift from Dr. W. Hillen, Erlangen University; Urlinger *et al.*, 2000). PGAP2 was induced with 0.05 μg/ml doxycycline (the lowest concentration able to fully recover the cell surface expression of GPI-APs) for 1 d and the cells were then cultured without doxycycline for another 1 d. Cells (1×10^8) were suspended in 1.5 ml of a buffer (9.6% sucrose, 20 mM HEPES-NaOH, pH 7.4, 10 μg/ml leupeptin, 10 μg/ml aprotinin, 1 mM phenylmethylsulfonyl fluoride [PMSF]) and destroyed by nitrogen cavitation (300 psi, 4°C, 30 min). The cell lysate was centrifuged at 10,000 rpm at 4°C for 10 min and the supernatant was placed on top of a continuous sucrose gradient (20–50%). After centrifugation at 35,000 rpm (SW41 rotor) at 4°C for 19 h, 1-ml fractions were collected from the top and analyzed by SDS-PAGE and Western blotting. The primary antibodies used were anti-human transferrin receptor (TfR; Zymed Laboratories, South San Francisco, CA), anti-caveolin-1 (BD Biosciences), anti-ribophorin II (Santa Cruz Biotechnology, Santa Cruz, CA), anti-KDEL receptor (Stressgen, Victoria, British Columbia, Canada), anti-syntaxin 6 (Stressgen), anti-GS27 (Stressgen), anti-GS28 (Stressgen), anti-DAF (IA10) and anti-PGAP2, whereas the secondary antibodies were horseradish peroxidase (HRP)-conjugated anti-mouse IgG, HRP-conjugated anti-rabbit IgG, and HRP-conjugated anti-goat IgG (all from Amersham Bioscience, Piscataway, NJ).

Pulse-Chase Metabolic Labeling

Cells (2×10^6) were pre-incubated for 30 min at 37°C in methionine- and cysteine-free DMEM (Invitrogen) containing 25 mM HEPES-NaOH, pH 7.5, and 10% dialyzed FCS, pulsed with 100 μCi/ml [^{35}S]methionine and [^{35}S]cysteine (Amersham Bioscience) for 10 min at 37°C and then chased after adding cold 0.7 mM methionine and 0.3 mM cysteine. After each chase period, the culture medium and cell lysate were prepared (see Supplementary Information). Both the lysates and culture media were incubated with a monoclonal anti-DAF antibody (IA10) and protein A-Sepharose (Amersham Bioscience) that had been precoated with a nonlabeled CHO-K1 cell lysate. Immunoprecipitates were separated by SDS-PAGE and detected using a BAS 1000 analyzer (Fujifilm, Tokyo, Japan).

LC/ESIMS/MS Analysis of the GPI Anchor of CD59 Secreted from AM-B Cells

We generated AM-B cells expressing CD59 with tandem His, FLAG, GST, and FLAG-tags at the N-terminus (HFGF-CD59). The expressed HFGF-CD59 was captured from the culture medium by glutathione Sepharose 4B (Amersham Bioscience) and eluted with a solution consisting of 20 mM reduced glutathione, 30 mM Tris, and 150 mM NaCl. The purified HFGF-CD59 was subjected to SDS-PAGE and extracted after in-gel digestion with trypsin. The extracted peptides were directly analyzed by LC/ESIMS/MS using a Shimadzu LC-10ADvp LC system and an ion trap mass spectrometer LCQ (Thermo Finnigan, Waltham, MA) equipped with an electrospray ion source. A Unison C18 (Imtakt, Kyoto, Japan) reverse phase nano LC column (0.1 × 150 mm, 3 μm) was used for chromatographic separation of the peptides. A gradient solvent system was used at a flow rate of 500 nl/min with splitting. The LC was equipped with a 2-μl sample loop, and 2 μl of the sample was loaded using a PAL auto sampler (CTC Analytics, Zwingen, Switzerland). The mobile phase consisted of acetonitrile/water (5:95) containing 0.05% formic acid (solvent A) and acetonitrile/H_2O (90:10) containing 0.05% formic acid (solvent B). The gradient conditions were 100% A for 0–10 min, followed by a linear gradient from 95%A/5% B to 40% A/60% B for 10–110 min. The mass spectrometer was operated in the positive ion mode with data-dependent MS/MS. The mass range of the instrument was set at m/z 400-1500, and a scan speed of 1000 Da/s was used. The ion spray voltage was set at 5500 V in the positive ion mode. Nitrogen was used as the curtain gas and helium was used as the collision gas.

TX-114 Partitioning

Cells were lysed in 1 ml of a buffer (10 mM Tris-HCl, pH 7.4, 150 mM NaCl, 5 mM EDTA, 10 μg/ml leupeptin, 10 μg/ml aprotinin, 1 mM PMSF) containing 2% TX-114 (Nakalai Tesque, Kyoto, Japan) for 15 min on ice. After centrifugation at 15,000 rpm at 4°C for 15 min, the supernatant was incubated for 10 min at 37°C. Samples were separated into aqueous and detergent phases by centrifugation at 5600 × *g* at 37°C for 7 min. After separation, aliquots of buffer and 12% TX-114 were added to the detergent and aqueous phases, respectively, such that all the fractions were under the same conditions.

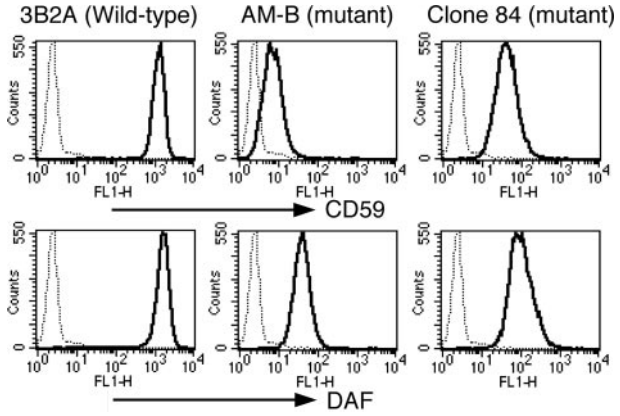

Figure 1. Decreased surface expressions of CD59 and DAF on the mutant cell lines AM-B and Clone 84. Wild-type 3B2A cells, mutant AM-B cells, and clone 84 cells were stained with anti-CD59 (top) and anti-DAF (bottom) antibodies and analyzed by flow cytometry. The dotted lines show negative control staining with isotype-matched IgG.

Separation of FLAG-mEGFP-GPI Using an Octyl-FF Column

3B2A and C84 cells (6×10^7) were transfected with pME-Neo2dH-VSVGts-FF-mEGFP-GPI. On the next day, the temperature was shifted to 40°C and the cells were cultured for a further 1 d. Next, the cells were chased under the indicated conditions. The 3B2A cells were incubated at 37°C for 5.5 h, washed twice with cold PBS, and then harvested by incubation in PBS containing 2 mM EDTA and 0.5% BSA on ice. The C84 cells were incubated for 4 h at 19.5°C and for 1.5 h at 37°C with 5 μg/ml BFA and then harvested as described above. The cell pellets were suspended in 5 ml of buffer A (60 mM 1-octyl-β-D-glucoside, 20 mM Tris-HCl, pH 7.4, 150 mM NaCl, 1 mM EDTA, 10 μg/ml leupeptin, 10 μg/ml aprotinin, 1 mM PMSF) and agitated for 1 h at 4°C. After centrifugation at 15,000 rpm at 4°C for 15 min, the supernatants were incubated with anti-FLAG (M2) beads overnight. The immunoprecipitates were washed twice with 0.5 ml of buffer B (30 mM 1-octyl-β-D-glucoside, 20 mM Tris-HCl, pH 7.4, 150 mM NaCl, 1 mM EDTA) and twice with 0.5 ml of buffer C (20 mM Tris-HCl, pH 7.4, 0.1% Nonidet P-40). FLAG-mEGFP-GPI was eluted with 100 μl of 0.1 M ammonium acetate containing 1 mg/ml FLAG-peptide (Sigma), 0.03% Nonidet P-40, and 5% 1-propanol four times (total volume, 400 μl). For phospholipase A_2 (PLA_2) treatment, immunoprecipitates bound to anti-FLAG beads obtained from 3B2A cell lysates were washed with buffers B and C, suspended in buffer D (100 mM Tris-HCl, pH 7.4, 6 mM $CaCl_2$, 0.1% Nonidet P-40, 10 μg/ml leupeptin, 10 μg/ml aprotinin, 1 mM PMSF) and treated with 75 U of PLA_2 (Sigma) at 37°C overnight. The beads were washed with buffers B and C, and PLA_2-treated FLAG-mEGFP-GPI was eluted as described above. A 200-μl aliquot of the eluate was loaded onto an Octyl-FF column (Amersham Bioscience) and chromatographed in ÄKTA (Amersham Bioscience) at a flow rate of 0.5 ml/min using a 5–40% gradient of 1-propanol. Fractions of 0.7 ml were collected, dried, subjected to SDS-PAGE, and analyzed by Western blotting using an anti-FLAG (M2) antibody and an HRP-conjugated anti-mouse IgG antibody.

Supplementary Data

Supplementary data are available at *MBC* online.

RESULTS

Characterization of Two Mutant Chinese Hamster Ovary Cell Lines with Defective Surface Expression of GPI-APs despite Normal Biosynthesis in the ER

We obtained two new mutant cell lines based on their defective surface expression of GPI-APs (see Supplementary Information for the establishment of these mutants). AM-B and Clone 84 (C84) cells, both derived from CHO cells expressing human CD59 and DAF (CD55) as a marker GPI-APs, showed partially deficient cell surface expressions of these molecules (Figure 1). Specifically, the CD59 and DAF expression levels on AM-B mutant cells were 0.7 and 2.9% of the wild-type levels, respectively, whereas the corresponding levels on C84 cells were 4.1 and 8.3% of the wild-type levels, respectively (Figure 1). The mutant phenotypes were not restored by transfection of any known genes involved in GPI-anchor biosynthesis (unpublished data). Moreover, GPI-anchor biosynthesis in these mutant cells was normal, because metabolic labeling experiments using [2-^{3}H]D-mannose, UDP-[6-^{3}H]GlcNAc, and *myo*-[2-^{3}H]inositol did not show any abnormal accumulation of GPI biosynthetic intermediates (unpublished data). Therefore, we concluded that C84 and AM-B cells were new mutants that were defective in a step occurring after biosynthesis of GPI-APs in the ER. The GPI-AP expressions on both C84 and AM-B cells were restored by transfection of a PGAP2 cDNA (Figure 2A; see below for the cloning of PGAP2), suggesting that they belong to the same mutant group.

To examine whether these defective surface expressions are common and specific to GPI-APs, several GPI-APs and TM proteins were expressed with or without PGAP2 in AM-B cells and their expressions were analyzed by FACS. We tested FLAG-tagged-CD59, FLAG-tagged-folate receptor, and PLAP as examples of GPI-APs, and FLAG-tagged-CD59-TM, IL2 receptor α, p75 (NGFR), and FLAG-tagged-VSVG as examples of TM proteins. The levels of all the GPI-APs were greatly diminished in the absence of PGAP2, whereas the TM proteins were expressed at comparable levels in the presence or absence of PGAP2 (Figure 2B). These data demonstrated that the defective surface expression was common and specific to GPI-APs.

Cloning and Characterization of PGAP2

We isolated a rat PGAP2 cDNA that restored the surface expression of CD59 on C84 cells by expression cloning and obtained hamster PGAP2 from a CHO cDNA library by PCR. Furthermore, we identified human PGAP2 with 95% amino acid identity to rat PGAP2 in the NR database (NCBI). The rat, hamster, and human PGAP2 cDNAs each encoded 254 amino acids (Figure 2C). Rat FGF receptor-activating gene 1 (FRAG1) (Lorenzi *et al.*, 1996) appeared to be identical to PGAP2, except for several C-terminal amino acids. Alternatively spliced PGAP2 cDNAs that lacked nucleotides encoding four amino acids (VSQE) were present in Chinese hamsters and humans (Figure 2C, ♦2). These shorter isoforms were functional, as assessed by their restoration of CD59 surface expression upon transfection into mutant cells (unpublished data).

We showed that PGAP2 was the gene responsible for the AM-B cell defect by mRNA analysis (Supplementary Figure 1).

Next, we analyzed the subcellular localization of PGAP2. Rabbit polyclonal anti-rat PGAP2 antibodies were raised against the C-terminal peptide. Because we were unable to detect endogenous PGAP2 protein, we transfected NRK cells with the rat PGAP2 cDNA and myc-tagged DPM2, an ER marker protein (Maeda *et al.*, 1998), followed by staining with anti-PGAP2 and anti-GM130 or anti-myc antibodies. PGAP2 was clearly stained in the Golgi identified by the Golgi matrix marker protein GM130 and to a lesser extent in the ER (Figure 3A). PGAP2 was not localized at the ER-Golgi intermediate compartment stained with anti-GS27 antibody (unpublished data). Brefeldin A (BFA) treatment, which is known to cause rapid redistribution of Golgi proteins into the ER, altered the localization of PGAP2 to the ER, where it colocalized with DPM2 (Figure 3A), confirming that PGAP2 was localized in the Golgi. Because PGAP2 was overexpressed in these experiments and overexpression can sometimes cause mislocalization of proteins, we repeated the

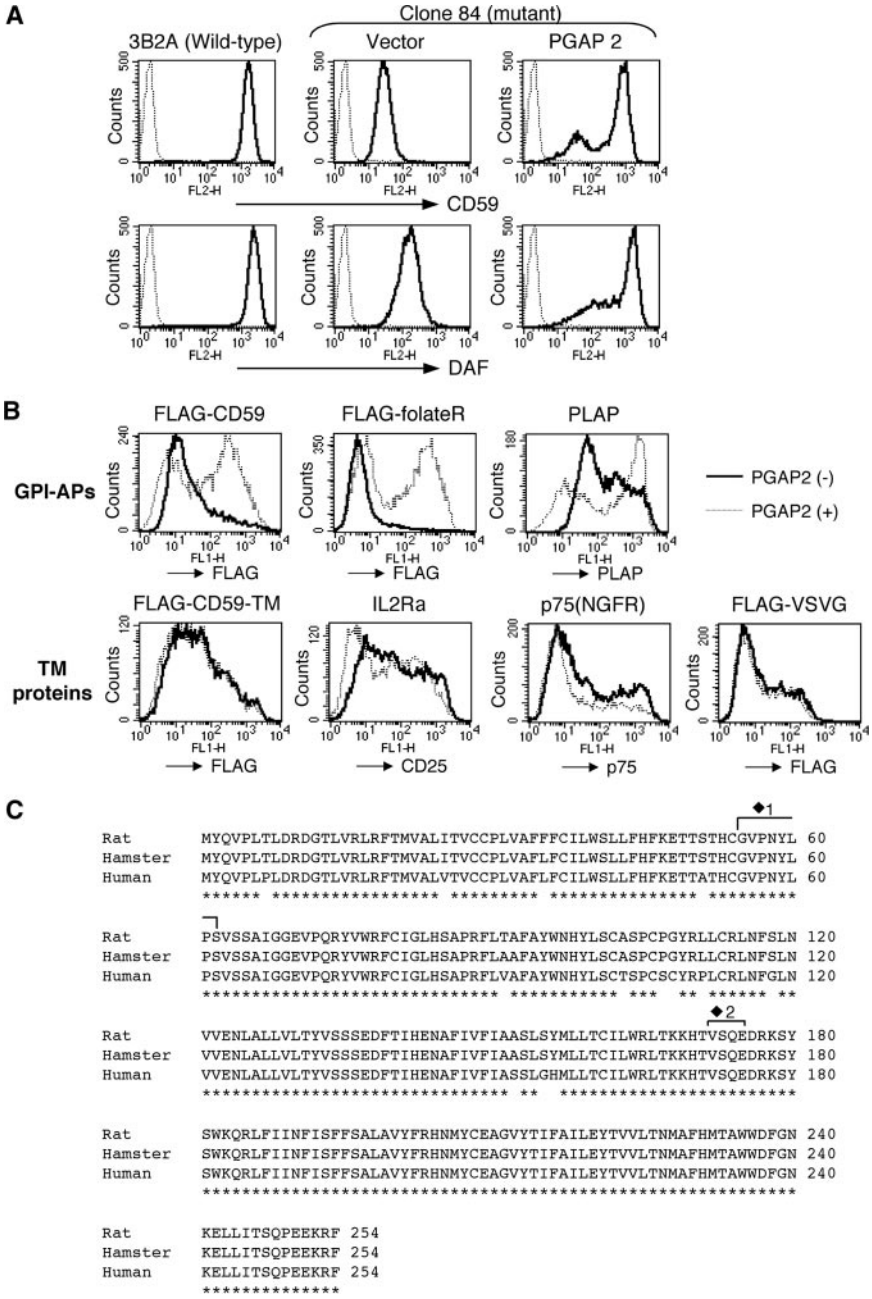

Figure 2. (A) Restoration of the surface expressions of CD59 and DAF after transfection of a PGAP2 cDNA. Mutant Clone 84 cells were transfected with a mock vector or PGAP2 cDNA expression vector. At 2 d after the transfection, the cells were stained with biotinylated anti-CD59 (top) and anti-DAF (bottom) antibodies followed by phycoerythrin-conjugated streptavidin. The dotted lines show negative control staining with the second reagent only. (B) Selective decrease in surface GPI-APs on the mutant cells. Mutant AM-B cells were cotransfected with the indicated plasmids and either a mock vector (bold lines) or PGAP2 expression vector (dotted lines). FLAG-tagged-CD59, FLAG-tagged-folate receptor, and PLAP are GPI-APs, whereas FLAG-tagged-CD59-TM, IL2 receptor α (IL2Rα), p75 (nerve growth factor receptor; NGFR), and FLAG-VSVG are transmembrane (TM) proteins. At 2 d after the transfection, the cells were stained with anti-FLAG, anti-PLAP, anti-IL2Rα, or anti-p75 antibodies. (C) Alignment of the amino acid sequences of PGAP2 homologues. Rat (GenBank Accession No. AB236144), Chinese hamster (Accession No. AB236145), and human (Accession No. AAQ75733) PGAP2s are aligned using the ClustalW software. The 22 nucleotides encoding the amino acids indicated by ◆1 are deleted in the mutant AM-B cells (see Supplementary Information). There is also an alternatively spliced form of PGAP2 that encodes a protein lacking the four amino acids indicated by ◆2.

analysis using the Tet-on system to regulate the expression of PGAP2. Even when the expression level was only slightly above the detection limit, the staining pattern did not change (unpublished data). Finally, we analyzed the localization of PGAP2 expressed at a low level under the Tet-on system by subcellular fractionation using sucrose-density gradient ultracentrifugation. PGAP2 fractionation was most similar to that of GS28, a *cis*-Golgi protein that recycles between the Golgi and ER or Golgi cisternae (Subramaniam *et al.*, 1996). The distribution of PGAP2 also partially coincided with ribophorin II, an ER protein (Figure 3B). Although quantitative measurement of the ratio of PGAP2 in the ER to that in the Golgi has been difficult, these results indicated that PGAP2 was expressed in the Golgi at a high density and in the ER at a lower density.

Low Surface Expression of GPI-APs Is Due to Rapid Secretion

To understand the basis of the low surface expressions of GPI-APs, we analyzed the stability and transport kinetics of GPI-APs by pulse-chase metabolic labeling experiments. DAF is highly O-glycosylated and sialylated during maturation in the Golgi (Lublin *et al.*, 1986), such that the ER form can be distinguished from the mature form by its molecular size. In mutant AM-B cells, DAF matured with glycosylation at a rate similar to that in wild-type BTP2 cells (AM-B cells permanently transfected with PGAP2). Subsequently, however, DAF was rapidly secreted from AM-B cells into the culture medium, whereas almost no DAF was secreted from BTP2 cells (Figure 4). These results showed that DAF was not degraded in the cells but secreted into the culture me-

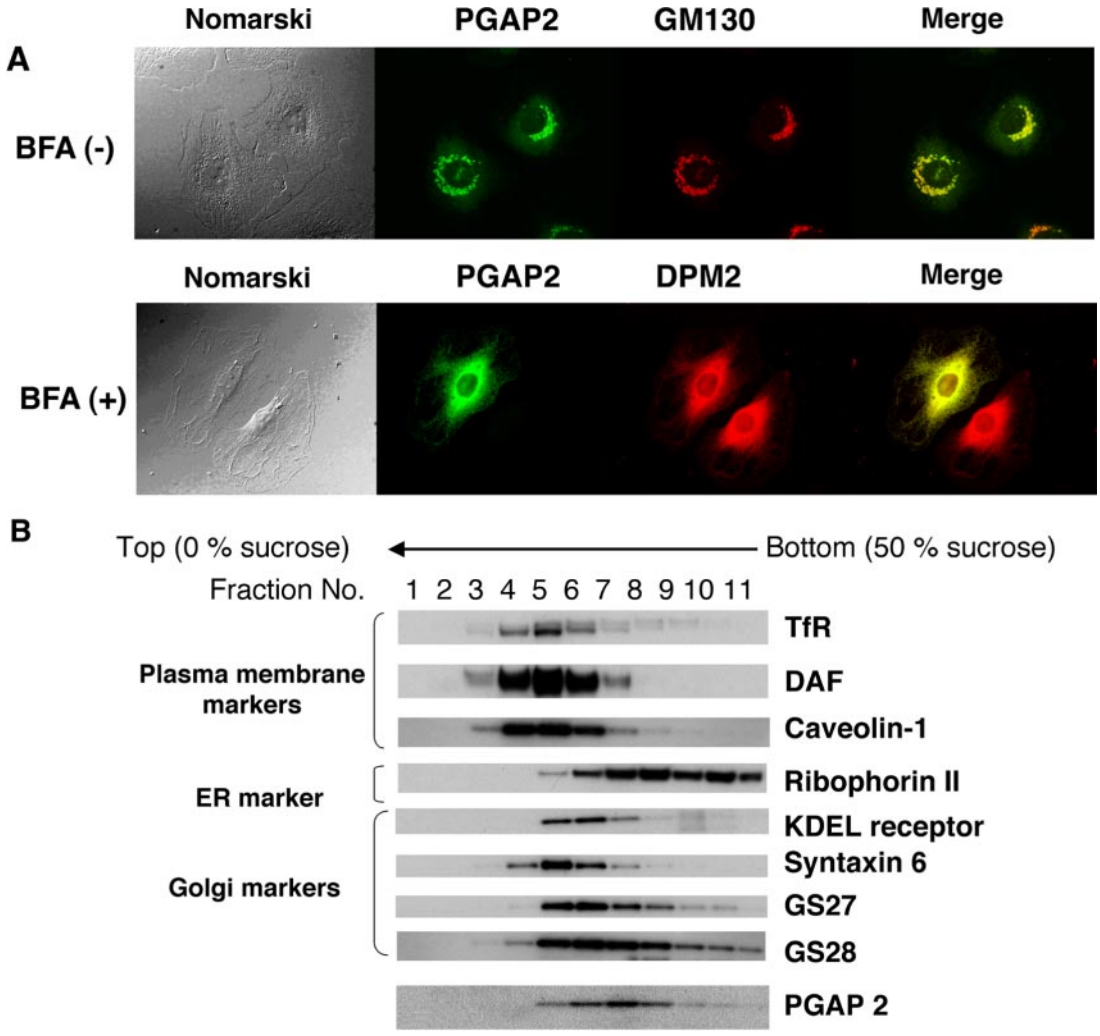

Figure 3. Subcellular localization of PGAP2. (A) NRK cells transfected with the rat PGAP2 cDNA and myc-tagged DPM2 were fixed, permeabilized with 0.1% TX-100, and double-stained with anti-PGAP2 and either anti-GM130 (top) or anti-myc (bottom) antibodies. The bottom panels show staining after treatment with BFA for 10 min. (B) PGAP2 was expressed in AM-B cells at the lowest concentration required for restoration of surface CD59 expression. The cell lysate was layered on top of a continuous sucrose gradient and centrifuged at 35,000 rpm at 4°C for 19 h. Fractions were collected and analyzed by SDS-PAGE and Western blotting.

dium, following normal transport kinetics from the ER to the Golgi and presumably to the plasma membrane. It was observed that the secreted DAF was smaller than the mature DAF. The molecular sizes of the secreted and cell-associated DAFs were almost identical after sialidase treatment (unpublished data), indicating that the decreased size was due to partial loss of sialic acids after secretion. CD59 was also secreted from AM-B cells into the medium (Supplementary Figure 2). These results indicated that the low surface expression of GPI-APs in PGAP2-deficient cells was due to secretion of GPI-APs into the medium.

Secretion of GPI-APs Is Due to Cleavage between Inositol and Phosphate

To examine whether the GPI-APs secreted from the mutant AM-B cells retained their GPI-anchor, we used *Clostridium*

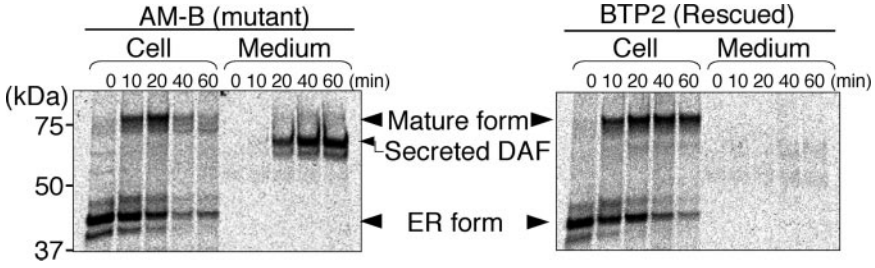

Figure 4. Pulse-chase metabolic labeling of GPI-APs. AM-B and BTP2 cells were pulsed with [^{35}S]methionine and [^{35}S]cysteine for 10 min and then chased for the indicated periods. The cell lysates and culture supernatants were immunoprecipitated with an anti-DAF antibody, separated by SDS-PAGE, and analyzed using a BAS 1000 analyzer.

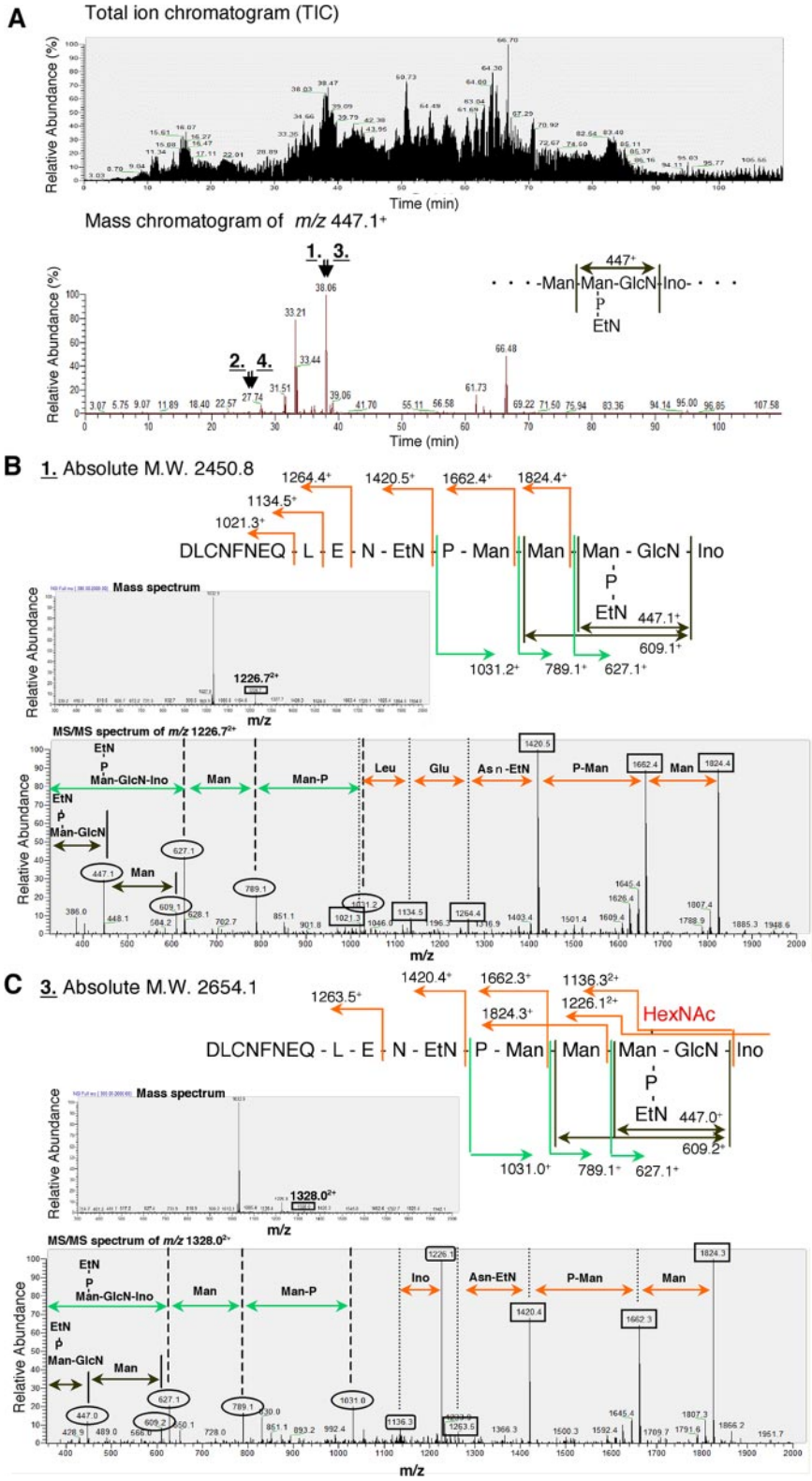

Figure 5. Secretion of GPI-APs by cleavage between inositol and phosphate. (A) HFGF-CD59 secreted from AM-B cells was digested with trypsin and analyzed by LC/ESIMS/MS. Top, the total ion chromatogram; bottom, a mass chromatogram of the molecular ions that generated a GPI-specific fragment ion of m/z 447^{+} in the MS/MS analysis. The molecular ions labeled 1–4 (peaks 1–4) correspond to C-terminal peptides bearing GPI. (B) MS/MS spectrum of the peak 1 ion of m/z 1226.7^{2+} and its determined structure. Top, the determined structure and the absolute mass; middle, first MS analysis of peak 1; bottom, the second MS of the parent fragment with m/z 1226.7^{2+} shown in the middle panel. The b-series fragments are indicated by orange arrows, and the terminal and internal fragments of GPI structure are indicated by green and gray arrows, respectively. The peak of 1032.9^{+} in the middle panel corresponded to an internal peptide, LTQSMAIIR, from HFGF-CD59. (C) MS/MS spectrum of the peak 3 ion of m/z 1328.0^{2+} and its determined structure. Panels are indicated similarly to B. The size difference of m/z between peaks 1 and 3 (101.3^{2+}) corresponded to *N*-acetylhexosamine (HexNAc) attached to the first mannose. Note that the parent fragments with m/z 1032.9^{+} and 1226.7^{2+} were also present in peak 3 (middle) because of insufficient separation of peak 3 from very close peak 1 in LC (A).

septicum α-toxin as a probe, because it is known to selectively bind to the GPI anchor (Gordon *et al.*, 1999; Hong *et al.*, 2002). DAF was precipitated by α-toxin from the culture medium of AM-B cells as efficiently as by an anti-DAF antibody (Supplementary Figure 3A). Furthermore, metabolic pulse labeling with [2-^{3}H]D-mannose confirmed that the CD59 secreted from AM-B cells retained its GPI anchor (Supplementary Figure 3B). These results indicated that GPI-APs secreted from PGAP2-defective mutant cells contained part of the GPI-anchor.

To determine the cleavage site within GPI, we analyzed the structures of the secreted GPI-APs using LC/ESIMS/

MS. We permanently transfected His-FLAG-GST-FLAG-tagged CD59 (HFGF-CD59) into AM-B cells, purified HFGF-CD59 secreted from the cells into the culture medium, and analyzed its structure by LC/ESIMS/MS after trypsin digestion. The molecular ions of the C-terminal peptide bearing GPI were screened by the presence of a GPI-specific collision fragment of m/z 447.1^{+} (ethanolamine phosphate-mannose-glucosamine) in the second MS. From the four peaks of such molecular ions (peaks 1–4 in Figure 5A), b-series fragments as well as fragments of the characteristic GPI-anchor structure were identified (Figure 5, B and C). On the basis of the m/z value 1226.7^{2+} of parent mass in the major peak 1 (middle panel in Figure 5B) and the profile of the fragment ions (bottom panel in Figure 5B), we determined that peak 1 was the C-terminal GPI-anchored peptide spanning the aspartic acid next to the most C-terminal lysine and inositol. The ion mass 2451.4 calculated from m/z 1226.7^{2+} was very close to the absolute mass 2450.8 (top panel in Figure 5B). Therefore, the tagged CD59 was released by the action of a phospholipase D (PLD). Peak 2 had an extra lysine due to cleavage between two successive lysines. Peaks 3 and 4 corresponded to peaks 1 and 2, respectively, but had an additional *N*-acetylhexosamine attached, presumably to the first mannose (Figure 5C and unpublished data). The mass size difference of 202.6 between 1226.7^{2+} and 1328.0^{2+} was very close to the mass of *N*-acetylhexosamine, and this type of modification has been reported previously (Homans *et al.*, 1988). These results indicated that the backbone structure of GPI was the same as the previously reported common structure of surface GPI-APs and that all four peaks were generated by hydrolysis between inositol and phosphate by phosphodiesterase activity, such as a PLD.

DAF Is Released from the Membrane at the Cell Surface

Next, we examined where GPI-APs are released from the membrane in the mutant cells. AM-B cells were metabolically labeled in the presence of BFA at 37°C to block transport beyond the mixed ER/Golgi system. Chases were performed under different conditions as indicated in the top panel of Figure 6A. TX-114 phase separation assays were used to distinguish membrane-bound GPI-APs from cleaved soluble GPI-APs. In the case of chasing at 37°C without BFA, the majority of DAF was secreted into the medium (Figure 6A, condition 2) and partitioned into the aqueous phase (unpublished data), as expected. During chasing for 1.5 h at 37°C in the presence of BFA, DAF was retained in the cells and partitioned into the detergent phase (condition 1) and no secretion was observed (unpublished data). Under condition 1, intracellular DAF seemed to be partially sialylated. To examine whether the cleavage/release occurred at the *trans*-Golgi network (TGN), chasing was performed at 19.5°C, which blocks transport from the TGN to the plasma membrane. Under this condition, mature DAF was partitioned into the detergent phase (condition 3). To eliminate the possibility that 19.5°C was too cold for the cleavage enzyme, the chase at 19.5°C was followed by incubation for 2 h at 37°C in the presence of BFA (condition 4; Miller *et al.*, 1992; Strous *et al.*, 1993). This incubation did not cause secretion of DAF into the culture medium and mature DAF was again partitioned into the detergent phase (condition 4). These data indicated that DAF was not released during transport from the ER to the TGN.

Next, we used tannic acid to examine whether the cleavage occurred during transport from the TGN to the plasma membrane. Tannic acid fixes the plasma membrane and inhibits vesicle fusion with the plasma membrane without affecting intracellular membranes and vesicle trafficking

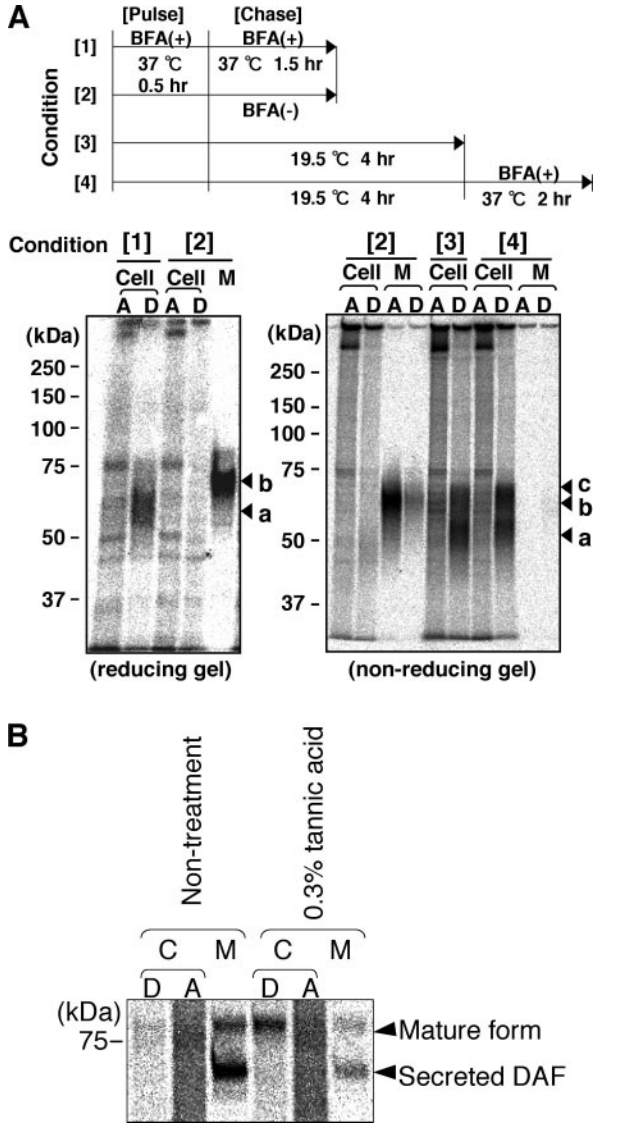

Figure 6. Release of DAF from the membrane at the cell surface. (A) AM-B cells were pulse-labeled with [^{35}S]methionine and [^{35}S]cysteine and chased under the four conditions shown in the top panel. A TX-114 partitioning assay was used to separate the soluble and membrane-bound proteins into aqueous and detergent phases, respectively. The chases under conditions that inhibit transport to the cell surface, such as in the presence of BFA (conditions 1 and 4) or incubation at 19.5°C (conditions 3 and 4), prevent the release of DAF, contrary to the normal condition (condition 2). Cell, cell lysate; M, medium; A, aqueous phase; D, detergent phase; a, premature form; b, secreted form; c, mature form. (B) After pulse-labeling with [^{35}S]methionine and [^{35}S]cysteine for 10 min, AM-B cells were chased with or without 0.3% tannic acid for 40 min. The cell lysates were phase-separated by TX-114 partitioning. C, cell lysate; M, medium; A, aqueous phase; D, detergent phase.

(Polishchuk *et al.*, 2004). After the pulse for metabolic labeling, AM-B cells were chased for 40 min in the absence or presence of tannic acid. In the presence of tannic acid, intracellular mature DAF was separated into the detergent phase, indicating that DAF was membrane-bound (Figure 6B). Taken together with the kinetics data showing that the secretion started soon after the arrival of DAF at the cell

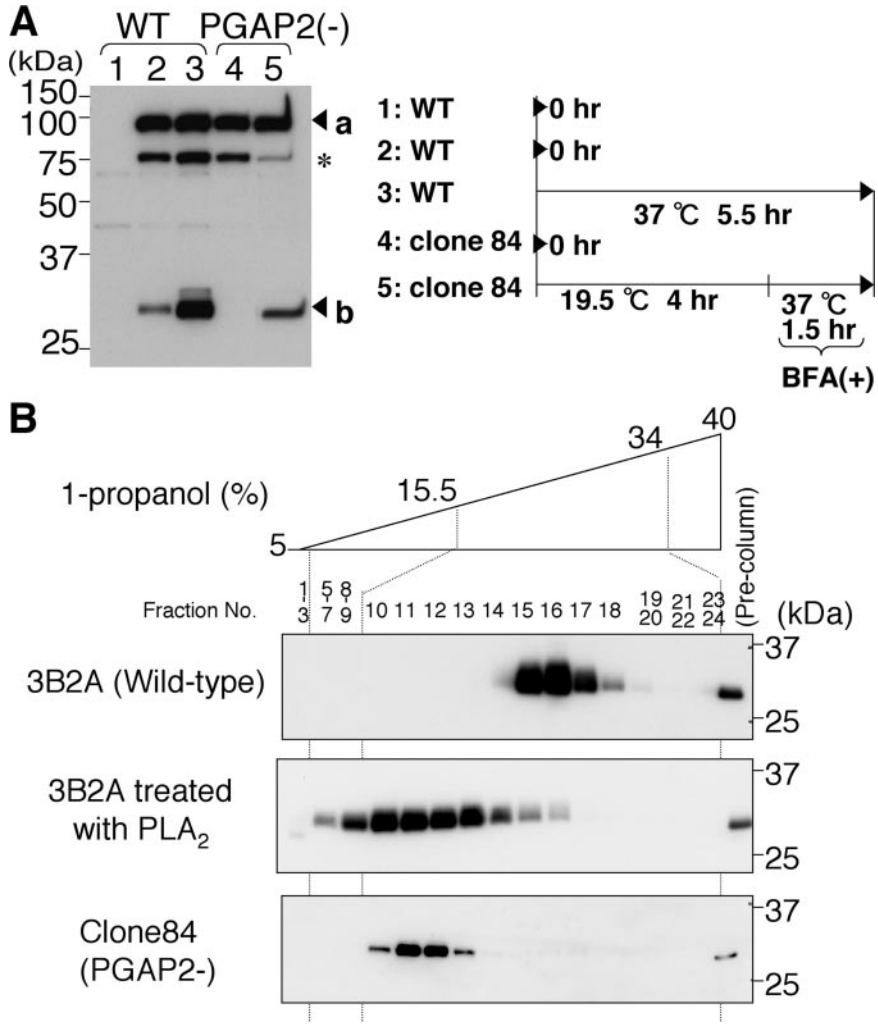

Figure 7. Intracellular processing of a reporter GPI-AP. (A) Wild-type 3B2A (lanes 1–3) and C84 (lanes 4 and 5) cells were transfected without (lane 1) or with (lanes 2–5) VSVGts-FF-mEGFP-GPI and cultured at 40°C for 1 d. Cells were further cultured under the conditions shown on the right. The cell lysates were immunoprecipitated with an anti-FLAG antibody, subjected to SDS-PAGE, and analyzed by Western blotting. a, VSVGts-FF-mEGFP-GPI; b, FLAG-mEGFP-GPI (a cleavage product of VSVGts-FF-mEGFP-GPI by furin); asterisk, a degradation product. (B) 3B2A and C84 cells transfected with VSVGts-FF-mEGFP-GPI were cultured under the same conditions shown in lanes 3 and 5 in A. FLAG-mEGFP-GPI was collected from the cell lysates with anti-FLAG beads and eluted with a FLAG-peptide. To prepare lyso-GPI-anchored FLAG-mEGFP-GPI, aliquots of the immunoprecipitates from 3B2A cells were treated with PLA_2. FLAG-mEGFP-GPIs were chromatographed in an Octyl-FF column with a 5–40% gradient of 1-propanol. Fractions were subjected to SDS-PAGE and analyzed by Western blotting with an anti-FLAG antibody.

surface (Figure 4), these results strongly suggested that DAF was released from the membrane at the cell surface of PGAP2-deficient cells.

Intracellular Processing of GPI Yields lyso-GPI-APs

To understand how deficiency in the Golgi/ER-resident PGAP2 leads to cleavage of GPI-APs at the cell surface, we assumed that GPI-APs arriving at the surface of PGAP2-defective cells have an aberrant GPI structure that is sensitive to a PLD. If this is true, the phosphatidic acid moiety of GPI must be abnormal because the glycan part of the secreted GPI-APs was normal (Figure 5). To analyze the structure of intracellular post-Golgi GPI-APs, we designed a temperature-sensitive chimeric reporter protein, whose exit from the ER was controllable by a temperature shift and whose transport to the TGN can be monitored by size changes. This reporter, VSVGts-FF-mEGFP-GPI, consisted of the extracellular domain of the temperature-sensitive vesicular stomatitis virus G protein (VSVGtsO45; Gallione and Rose, 1985), a furin cleavage site (Nakayama, 1997), a FLAG tag, modified EGFP, and a GPI attachment signal. Because of the temperature-sensitivity of the extracellular domain of VSVGtsO45, the reporter protein was retained in the ER at 40°C and only left the ER for transport to the TGN once the temperature was shifted to a permissive temperature below 32°C, although the temperature restriction and exit efficiency from the ER were not as good as those of full-length VSVGtsO45 (our unpublished observations). In the TGN, furin cleaved the 90-kDa reporter protein to yield a smaller protein of 30 kDa, FLAG-mEGFP-GPI, such that the post-Golgi reporter protein could be distinguished from the ER/Golgi-localized protein (Figure 7A, lane 3). To allow accumulation of the furin-cleaved reporter protein in the TGN in C84 cells, incubation at 19.5°C for 4 h that allowed transport to the TGN but inhibited exit from the TGN, was followed by incubation for 1.5 h at 37°C in the presence of BFA for complete proteolysis by furin (Figure 7A, lane 5). FLAG-mEGFP-GPIs accumulated in C84 cells and expressed on the surface of wild-type cells were collected using anti-FLAG antibody-conjugated beads. We analyzed the hydrophobicity of the proteins by fractionation in octyl-Sepharose using elution with a 1-propanol gradient. Wild-type FLAG-mEGFP-GPI harboring two lipid chains was eluted in fractions 15–18 (Figure 7B, top panel). Lyso-GPI harboring one lipid chain prepared from wild-type FLAG-mEGFP-GPI by PLA_2 treatment was eluted in fractions 8–14 (middle panel). FLAG-mEGFP-GPI from C84 cells (bottom panel) was eluted in similar fractions to the PLA_2-treated lyso-GPI but clearly different fractions from wild-type GPI, strongly suggesting that the FLAG-mEGFP-GPI in PGAP2-deficient cells had one lipid chain. The amount of FLAG-mEGFP-GPI from C84 cells was not sufficient to determine its structure by MS

analysis. These results suggested that lyso-GPI-APs were produced by a putative Golgi/ER-resident PLA in the absence of PGAP2, transported to the cell surface, cleaved by a PLD and secreted.

DISCUSSION

In the present study, we established new mutant cell lines in which the surface expression of GPI-APs was greatly decreased despite normal GPI-APs biosynthesis in the ER. Furthermore, we identified a gene responsible for this defect by expression cloning and designated it PGAP2. To the best of our knowledge, this is the first protein localized in organelles other than the ER that has been shown to affect the processing of GPI-APs in mammalian cells. In our mutant cells, GPI-APs were modified/cleaved in two sequential reaction steps at different organelles. Less hydrophobic GPI-APs, most likely harboring lyso-GPI, were produced before their arrival at the plasma membrane, and soluble GPI-APs were subsequently produced at the cell surface by a putative PLD.

Characteristics of PGAP2

PGAP2 encoded a protein of 254 or 250 amino acids. Rat PGAP2 appeared to be identical to FRAG1 (Lorenzi *et al.*, 1996). In a rat osteosarcoma cell line, chromosomal rearrangement produced a fusion protein of fibroblast growth factor receptor 2 and FRAG1 with constitutively elevated tyrosine kinase activity. Because PGAP2 does not contain any known domains, it is difficult to predict its functions from the amino acid sequence. PGAP2s are conserved among eukaryotes. The PGAP2 homologue in *Saccharomyces cerevisiae*, Cwh43p, is much larger than mammalian PGAP2 and has an extradomain of ~700 amino acids (Martin-Yken *et al.*, 2001). The yeast mutant *cwh43-2*, originally isolated for its Calcofluor White hypersensitivity, displays several cell wall defects, which notably include increased release of β-1,6-glucan, Cwp1p, which is a GPI-AP, and Pir2p, which is covalently attached to the cell wall (Martin-Yken *et al.*, 2001). Because many GPI-APs, such as Cwp1p, Cwp2p, Gas1p, and Dcw1p, are involved in cell wall biogenesis (Kitagaki *et al.*, 2002; Frieman and Cormack, 2003), we assume that the secretion of GPI-APs from the *cwh43-2* yeast mutant occurs in a manner similar to that in our PGAP2-deficient cells, thereby resulting in defective cell wall biogenesis.

Candidate PLD Acting on GPI-APs

We showed that the GPI-APs in our PGAP2-deficient cells were subjected to sequential modifications/cleavages in intracellular organelles and on the plasma membrane. The first event, namely intracellular modification/cleavage, is most likely to occur in the Golgi, because most of the PGAP2 protein is localized in the Golgi. The second event, namely digestion by a PLD on the plasma membrane, must be dependent on the first event, because such rapid and efficient cleavage was not observed in normal cells. The substrate of the PLD appeared to be lyso-GPI. The basis for why the second event only occurs in PGAP2-deficient cells may be that the PLD cleaves lyso-GPI-APs but not normal GPI-APs. Alternatively, normal GPI-APs localized in rafts may be prevented from encountering the PLD, whereas lyso-GPI-APs may lose their specific localization and be susceptible to the cleavage. GPI-PLD is the only enzyme known to cleave GPI-APs and exists abundantly in serum. It is known that GPI-PLD cannot act on surface GPI-APs under physiological conditions (Scallon *et al.*, 1991; Deeg and Davitz, 1995). We examined whether GPI-PLD present in FCS was responsible for the second event. The secretion of DAF was slower under serum-free conditions and the addition of FCS or recombinant GPI-PLD to the serum-free medium accelerated the secretion (our unpublished results). However, PGAP2-deficient cells cultured in serum-free medium for more than 1 mo showed only a small increase in the surface expression of GPI-APs (our unpublished results). Moreover, bathophenanthroline, a membrane-impermeable inhibitor of GPI-PLD, did not inhibit the secretion of DAF (our unpublished results). These results clearly indicate that another PLD that cleaves lyso-GPI must be expressed in CHO cells. Recently, it was reported that enzymes in a family of nucleotide pyrophosphatases/phosphodiesterases have lyso-PLD activity that is resistant to metal-chelating reagents, such as bathophenanthroline (Scallon *et al.*, 1991; Tokumura *et al.*, 2002), although whether these enzymes cleave lyso-GPI-APs has not yet been determined.

Possible Lipid Remodeling of GPI and PGAP2

How does PGAP2 deficiency cause the first event? We consider that this point can be discussed in terms of the lipid remodeling of GPI. Both 1-alkyl, 2-acyl PI, and diacyl PI are used in mammalian GPI-APs and in both cases two saturated alkyl/acyl chains are usually involved. In particular, a stearoyl (C18:0) group is mainly used in the *sn*-2 position (McConville and Ferguson, 1993; Brewis *et al.*, 1995; Treumann *et al.*, 1995; Ikezawa, 2002). Saturated chains are compatible with the liquid ordered phase of rafts in which GPI-APs are enriched (Schroeder *et al.*, 1994; Ahmed *et al.*, 1997; Subczynski and Kusumi, 2003). In contrast, intracellular PI, from which GPI is synthesized, usually has an unsaturated chain in the *sn*-2 position and the major species is *sn*-1-stearoyl (C18:0)-*sn*-2-arachidonoyl (C20:4)-PI (Kerwin *et al.*, 1994). On the basis of the structural differences between free PI and PI in GPI-APs, we propose that lipid remodeling occurs in GPI-APs in mammalian cells. Lipid remodeling of GPI is well known to occur in *S. cerevisiae* (Reggiori *et al.*, 1997; Sipos *et al.*, 1997) and *Trypanosoma brucei* (Masterson *et al.*, 1990; Morita *et al.*, 2000; Morita and Englund, 2001). In *S. cerevisiae*, diacylglycerol-containing GPI is remodeled into ceramide-containing GPI or, in some cases, into diacylglycerol with a long fatty acyl chain (C26:0) in the *sn*-2 position (Reggiori *et al.*, 1997; Sipos *et al.*, 1997). In *T. brucei*, GPIs of variant surface glycoproteins have been well characterized and their lipid moieties are converted to dimyristoyl-PI by putative remodelases with PLA-like activity before attachment to the proteins (Morita *et al.*, 2000). Although little is known about the precise mechanism, exchange of the *sn*-2 acyl chain occurs in both organisms. We assume a similar reaction may occur in mammalian cells, such that the unsaturated *sn*-2 acyl chain is replaced by a saturated acyl chain. In this process, PGAP2 and a putative PLA may cooperate as the remodelase and a defect in PGAP2 may cause cleavage by PLA without replacement of the chain. Further studies are required to test these possibilities.

Secretion of GPI-anchored NCAMs during Differentiation of Myoblasts

A previous study reported that GPI-anchored NCAMs expressed on the myoblast cell line C2C12 were released from the cell surface during myoblast differentiation (Mukasa *et al.*, 1995). This release was observed even when the cells were cultured in the absence of FCS and was resistant to EDTA and phenanthroline. Moreover, the secretion was catalyzed by PLD-like cleavage. This situation is quite similar to that seen in our PGAP2-deficient cells. Although the

biological significance of the secretion of GPI-anchored NCAMs remains unresolved, it is very interesting to examine whether the secretion is caused by down-regulation of PGAP2. We could not detect any endogenous PGAP2 in C2C12 cells by either Western blotting or immunofluorescence microscopy with polyclonal antibodies (our unpublished results). These findings may reflect that PGAP2 is not abundant and therefore that its down-regulation may mimic the situation of PGAP2-deficiency. Future studies investigating whether the expression of PGAP2 is regulated and whether overexpression of PGAP2 disturbs the differentiation of C2C12 cells will provide clues for how PGAP2 works in vivo.

ACKNOWLEDGMENTS

We thank Fumiko Ishii and Keiko Kinoshita for excellent technical assistance and Kohjiro Nakamura for help with the cell sorting. This work was supported by grants from the Ministry of Education, Culture, Sports, Science, and Technology of Japan and the Core Research for Evolutional Science and Technology, Japan Science and Technology Agency.

REFERENCES

Ahmed, S. N., Brown, D. A., and London, E. (1997). On the origin of sphingolipid/cholesterol-rich detergent-insoluble cell membranes: physiological concentrations of cholesterol and sphingolipid induce formation of a detergent-insoluble, liquid-ordered lipid phase in model membranes. Biochemistry *36*, 10944–10953.

Brewis, I. A., Ferguson, M. A., Mehlert, A., Turner, A. J., and Hooper, N. M. (1995). Structures of the glycosyl-phosphatidylinositol anchors of porcine and human renal membrane dipeptidase. Comprehensive structural studies on the porcine anchor and interspecies comparison of the glycan core structures. J. Biol. Chem. *270*, 22946–22956.

Brown, D. A., and Rose, J. K. (1992). Sorting of GPI-anchored proteins to glycolipid-enriched membrane subdomains during transport to the apical cell surface. Cell *68*, 533–544.

Chatterjee, S., Smith, E. R., Hanada, K., Stevens, V. L., and Mayor, S. (2001). GPI anchoring leads to sphingolipid-dependent retention of endocytosed proteins in the recycling endosomal compartment. EMBO J. *20*, 1583–1592.

Cheong, K. H., Zacchetti, D., Schneeberger, E. E., and Simons, K. (1999). VIP17/MAL, a lipid raft-associated protein, is involved in apical transport in MDCK cells. Proc. Natl. Acad. Sci. USA *96*, 6241–6248.

Deeg, M. A., and Davitz, M. A. (1995). Glycosylphosphatidylinositol-phospholipase D: a tool for glycosylphosphatidylinositol structural analysis. Methods J. Biol. Chem. *250*, 630–640.

Ferguson, M. A. (1999). The structure, biosynthesis and functions of glycosylphosphatidylinositol anchors, and the contributions of trypanosome research. J. Cell Sci. *112*, 2799–2809.

Frieman, M. B., and Cormack, B. P. (2003). The omega-site sequence of glycosylphosphatidylinositol-anchored proteins in *Saccharomyces cerevisiae* can determine distribution between the membrane and the cell wall. Mol. Microbiol. *50*, 883–896.

Gallione, C. J., and Rose, J. K. (1985). A single amino acid substitution in a hydrophobic domain causes temperature-sensitive cell-surface transport of a mutant viral glycoprotein. J. Virol. *54*, 374–382.

Gordon, V. M., Nelson, K. L., Buckley, J. T., Stevens, V. L., Tweten, R. K., Elwood, P. C., and Leppla, S. H. (1999). *Clostridium septicum* alpha toxin uses glycosylphosphatidylinositol-anchored protein receptors. J. Biol. Chem. *274*, 27274–27280.

Hirt, B. (1967). Selective extraction of Polyoma DNA from infected mouse cell cultures. J. Mol. Biol. *26*, 365–369.

Homans, S. W., Ferguson, M. A., Dwek, R. A., Rademacher, T. W., Anand, R., and Williams, A. F. (1988). Complete structure of the glycosyl phosphatidylinositol membrane anchor of rat brain Thy-1 glycoprotein. Nature *333*, 269–272.

Hong, Y., Ohishi, K., Inoue, N., Kang, J. Y., Shime, H., Horiguchi, Y., van der Goot, F. G., Sugimoto, N., and Kinoshita, T. (2002). Requirement of *N*-glycan on GPI-anchored proteins for efficient binding of aerolysin but not *Clostridium septicum* α-toxin. EMBO J. *21*, 5047–5056.

Ikezawa, H. (2002). Glycosylphosphatidylinositol (GPI)-anchored proteins. Biol. Pharm. Bull. *25*, 409–417.

Kerwin, J. L., Tuininga, A. R., and Ericsson, L. H. (1994). Identification of molecular species of glycerophospholipids and sphingomyelin using electrospray mass spectrometry. J. Lipid Res. *35*, 1102–1114.

Kinoshita, T., and Inoue, N. (2000). Dissecting and manipulating the pathway for glycosylphosphatidylinositol-anchor biosynthesis. Curr. Opin. Chem. Biol. *4*, 632–638.

Kitagaki, H., Wu, H., Shimoi, H., and Ito, K. (2002). Two homologous genes, DCW1 (YKL046c) and DFG5, are essential for cell growth and encode glycosylphosphatidylinositol (GPI)-anchored membrane proteins required for cell wall biogenesis in *Saccharomyces cerevisiae*. Mol. Microbiol. *46*, 1011–1022.

Lorenzi, M. V., Horii, Y., Yamanaka, R., Sakaguchi, K., and Miki, T. (1996). FRAG1, a gene that potently activates fibroblast growth factor receptor by C-terminal fusion through chromosomal rearrangement. Proc. Natl. Acad. Sci. USA *93*, 8956–8961.

Lublin, D. M., Krsek-Staples, J., Pangburn, M. K., and Atkinson, J. P. (1986). Biosynthesis and glycosylation of the human complement regulatory protein decay-accelerating factor. J. Immunol. *137*, 1629–1635.

Maeda, Y., Tomita, S., Watanabe, R., Ohishi, K., and Kinoshita, T. (1998). DPM2 regulates biosynthesis of dolichol phosphate-mannose in mammalian cells: correct subcellular localization and stabilization of DPM1, and binding of dolichol phosphate. EMBO J. *17*, 4920–4929.

Martin-Belmonte, F., Puertollano, R., Millan, J., and Alonso, M. A. (2000). The MAL proteolipid is necessary for the overall apical delivery of membrane proteins in the polarized epithelial Madin-Darby canine kidney and Fischer rat thyroid cell lines. Mol. Biol. Cell *11*, 2033–2045.

Martin-Yken, H., Dagkessamanskaia, A., De Groot, P., Ram, A., Klis, F., and Francois, J. (2001). *Saccharomyces cerevisiae* YCRO17c/CWH43 encodes a putative sensor/transporter protein upstream of the BCK2 branch of the PKC1-dependent cell wall integrity pathway. Yeast *18*, 827–840.

Masterson, W. J., Raper, J., Doering, T. L., Hart, G. W., and Englund, P. T. (1990). Fatty acid remodeling: a novel reaction sequence in the biosynthesis of trypanosome glycosyl phosphatidylinositol membrane anchors. Cell *62*, 73–80.

Mayor, S., and Riezman, H. (2004). Sorting GPI-anchored proteins. Nat. Rev. Mol. Cell Biol. *5*, 110–120.

Mayor, S., Sabharanjak, S., and Maxfield, F. R. (1998). Cholesterol-dependent retention of GPI-anchored proteins in endosomes. EMBO J. *17*, 4626–4638.

McConville, M. J., and Ferguson, M. A. (1993). The structure, biosynthesis and function of glycosylated phosphatidylinositols in the parasitic protozoa and higher eukaryotes. Biochem. J. *294*(Pt 2), 305–324.

Miller, S. G., Carnell, L., and Moore, H. H. (1992). Post-Golgi membrane traffic: brefeldin A inhibits export from distal Golgi compartments to the cell surface but not recycling. J. Cell Biol. *118*, 267–283.

Morita, Y. S., Acosta-Serrano, A., Buxbaum, L. U., and Englund, P. T. (2000). Glycosyl phosphatidylinositol myristoylation in African trypanosomes. New intermediates in the pathway for fatty acid remodeling. J. Biol. Chem. *275*, 14147–14154.

Morita, Y. S., and Englund, P. T. (2001). Fatty acid remodeling of glycosyl phosphatidylinositol anchors in *Trypanosoma brucei*: incorporation of fatty acids other than myristate. Mol. Biochem. Parasitol. *115*, 157–164.

Morsomme, P., Prescianotto-Baschong, C., and Riezman, H. (2003). The ER v-SNAREs are required for GPI-anchored protein sorting from other secretory proteins upon exit from the ER. J. Cell Biol. *162*, 403–412.

Morsomme, P., and Riezman, H. (2002). The Rab GTPase Ypt1p and tethering factors couple protein sorting at the ER to vesicle targeting to the Golgi apparatus. Dev. Cell *2*, 307–317.

Mukasa, R., Umeda, M., Endo, T., Kobata, A., and Inoue, K. (1995). Characterization of glycosylphosphatidylinositol (GPI)-anchored NCAM on mouse skeletal muscle cell line C2C12, the structure of the GPI glycan and release during myogenesis. Arch Biochem. Biophys. *318*, 182–190.

Muniz, M., Nuoffer, C., Hauri, H. P., and Riezman, H. (2000). The Emp24 complex recruits a specific cargo molecule into endoplasmic reticulum-derived vesicles. J. Cell Biol. *148*, 925–930.

Nakamura, N., Inoue, N., Watanabe, R., Takahashi, M., Takeda, J., Stevens, V. L., and Kinoshita, T. (1997). Expression cloning of PIG-L, a candidate N-acetylglucosaminyl-phosphatidylinositol deacetylase. J. Biol. Chem. *272*, 15834–15840.

Nakayama, K. (1997). Furin: a mammalian subtilisin/Kex2p-like endoprotease involved in processing of a wide variety of precursor proteins. Biochem. J. *327*(Pt 3), 625–635.

Paladino, S., Sarnataro, D., Pillich, R., Tivodar, S., Nitsch, L., and Zurzolo, C. (2004). Protein oligomerization modulates raft partitioning and apical sorting of GPI-anchored proteins. J. Cell Biol. *167*, 699–709.

Polishchuk, R., Di Pentima, A., and Lippincott-Schwartz, J. (2004). Delivery of raft-associated, GPI-anchored proteins to the apical surface of polarized MDCK cells by a transcytotic pathway. Nat. Cell Biol. *6*, 297–307.

Reggiori, F., Canivenc-Gansel, E., and Conzelmann, A. (1997). Lipid remodeling leads to the introduction and exchange of defined ceramides on GPI proteins in the ER and Golgi of *Saccharomyces cerevisiae.* EMBO J. *16*, 3506–3518.

Scallon, B. J., Fung, W. J., Tsang, T. C., Li, S., Kado-Fong, H., Huang, K. S., and Kochan, J. P. (1991). Primary structure and functional activity of a phosphatidylinositol-glycan-specific phospholipase D. Science *252*, 446–448.

Schimmoller, F., Singer-Kruger, B., Schroder, S., Kruger, U., Barlowe, C., and Riezman, H. (1995). The absence of Emp24p, a component of ER-derived COPII-coated vesicles, causes a defect in transport of selected proteins to the Golgi. EMBO J. *14*, 1329–1339.

Schroeder, R., London, E., and Brown, D. (1994). Interactions between saturated acyl chains confer detergent resistance on lipids and glycosylphosphatidylinositol (GPI)-anchored proteins: GPI-anchored proteins in liposomes and cells show similar behavior. Proc. Natl. Acad. Sci. USA *91*, 12130–12134.

Simons, K., and Ikonen, E. (1997). Functional rafts in cell membranes. Nature *387*, 569–572.

Simons, K., and Toomre, D. (2000). Lipid rafts and signal transduction. Nat. Rev. Mol. Cell Biol. *1*, 31–39.

Sipos, G., Reggiori, F., Vionnet, C., and Conzelmann, A. (1997). Alternative lipid remodelling pathways for glycosylphosphatidylinositol membrane anchors in *Saccharomyces cerevisiae.* EMBO J. *16*, 3494–3505.

Skrzypek, M., Lester, R. L., and Dickson, R. C. (1997). Suppressor gene analysis reveals an essential role for sphingolipids in transport of glycosylphosphatidylinositol-anchored proteins in *Saccharomyces cerevisiae.* J. Bacteriol. *179*, 1513–1520.

Sotgia, F. *et al.* (2002). Intracellular retention of glycosylphosphatidyl inositol-linked proteins in caveolin-deficient cells. Mol. Cell Biol. *22*, 3905–3926.

Strous, G. J., van Kerkhof, P., van Meer, G., Rijnboutt, S., and Stoorvogel, W. (1993). Differential effects of brefeldin A on transport of secretory and lysosomal proteins. J. Biol. Chem. *268*, 2341–2347.

Subczynski, W. K., and Kusumi, A. (2003). Dynamics of raft molecules in the cell and artificial membranes: approaches by pulse EPR spin labeling and single molecule optical microscopy. Biochim. Biophys. Acta *1610*, 231–243.

Subramaniam, V. N., Peter, F., Philp, R., Wong, S. H., and Hong, W. (1996). GS28, a 28-kilodalton Golgi SNARE that participates in ER-Golgi transport. Science *272*, 1161–1163.

Sutterlin, C., Doering, T. L., Schimmoller, F., Schroder, S., and Riezman, H. (1997). Specific requirements for the ER to Golgi transport of GPI-anchored proteins in yeast. J. Cell Sci. *110*(Pt 21), 2703–2714.

Tanaka, S., Maeda, Y., Tashima, Y., and Kinoshita, T. (2004). Inositol deacylation of glycosylphosphatidylinositol-anchored proteins is mediated by mammalian PGAP1 and yeast Bst1p. J. Biol. Chem. *279*, 14256–14263.

Tokumura, A., Majima, E., Kariya, Y., Tominaga, K., Kogure, K., Yasuda, K., and Fukuzawa, K. (2002). Identification of human plasma lysophospholipase D, a lysophosphatidic acid-producing enzyme, as autotaxin, a multifunctional phosphodiesterase. J. Biol. Chem. *277*, 39436–39442.

Treumann, A., Lifely, M. R., Schneider, P., and Ferguson, M. A. (1995). Primary structure of CD52. J. Biol. Chem. *270*, 6088–6099.

Urlinger, S., Baron, U., Thellmann, M., Hasan, M. T., Bujard, H., and Hillen, W. (2000). Exploring the sequence space for tetracycline-dependent transcriptional activators: novel mutations yield expanded range and sensitivity. Proc. Natl. Acad. Sci. USA *97*, 7963–7968.